Research Article

Green Diesel Production Through Deoxygenation Reaction with Natural Zeolite-supported Nickel and Copper Catalyst

Gede Herry Arum Wijaya and Fidelis Stefanus Hubertson Simanjuntak*
Department of Renewable Energy Engineering, Universitas Prasetiya Mulya, BSD City Kavling Edutown I.1, Tangerang, Indonesia

Adid Adep Dwiatmoko
Research Center for Chemistry, National Research and Innovation Agency (BRIN), Kawasan Puspiptek, Serpong, South Tangerang, Indonesia

* Corresponding author. E-mail: fidelis.simanjuntak@prasetiyamulya.ac.id DOI: 10.14416/j.asep.2024.10.002
Received: 14 July 2024; Revised: 5 September 2024; Accepted: 25 September 2024; Published online: 7 October 2024

Abstract
The depletion of fossil fuels and their environmental impact necessitate sustainable alternatives. Green diesel, a biofuel with a chemical structure similar to conventional diesel, has gained traction as a viable alternative. This study explores the development of a cost-effective catalyst for green diesel production using deoxygenation. Deoxygenation refers to a broad class of chemical reactions where oxygen atoms are stripped from a molecule. This research employed abundant Indonesian natural zeolite (NZ) as a catalyst support, impregnated with non-noble metals, nickel (Ni), and copper (Cu). The investigation revealed that the NiCu/NZ catalyst achieved the highest oleic acid conversion (90.40%) and green diesel yield. The product distribution, ranging from C_{15} to C_{18} hydrocarbons, reflects the moderate acidity of the catalyst, promoting diverse cracking patterns compared to highly acidic catalysts. Additionally, the high specific surface area of NZ facilitates the conversion and good product distribution. Furthermore, the optimization process demonstrated that increasing hydrogen pressure during deoxygenation enhances both conversion rate and green diesel production.

Keywords: Copper, Deoxygenation, Green diesel, Natural zeolite, Nickel, Renewable energy

1 Introduction

A strong correlation exists between global economic growth and rising energy consumption. The majority of the energy used today comes from fossil energy sources. Diesel fuel is a type of fuel produced from crude oil and has an important role in the transportation sector. Fossil fuels are continuously depleted and the use of fossil fuels produces greenhouse gas emissions that can cause global warming. The search for sustainability has driven the development of environmentally friendly and renewable alternatives to fossil-fuel-derived diesel. Biodiesel, a renewable liquid fuel, derives from triglycerides reacting with alcohol via transesterification or esterification [1]. However, biodiesel has oxygen content in its compounds which can cause increased corrosive properties when stored for a long time [2]. In addition, biodiesel has a high acidity and a lower heating value than diesel [3], [4]. Therefore, biodiesel needs to be mixed with fossil fuels in the form of diesel as already known in Indonesia as B20 or B30. Based on this problem, an alternative biofuel production process is needed to produce higher quality diesel fuel.

Green diesel or diesel-like hydrocarbon is a renewable diesel fuel whose compound structure is similar to diesel from fossil fuels. Green diesel originates from renewable feedstocks, including triglycerides and their derivatives like fatty acids. Deoxygenation (DO) of vegetable oil has been developed as a green diesel production process today. DO is a type of (hydro)processing of vegetable raw

materials to produce hydrocarbons in the absence of oxygen. Deoxygenation includes all reactions that involve the removal of oxygen from a molecule such as hydrodeoxygenation (HDO), decarbonylation (deCO), and decarboxylation ($deCO_2$). Research related to the deoxygenation process using a model compound to find the best type of catalyst to produce green diesel is still in the development stage. Vegetable oils, including palm, castor, rapeseed, sunflower, and soybean, are rich sources of oleic acid, one of the most abundant fatty acids [5]. Oleic acid is an unsaturated compound that is very suitable for the deoxygenation process, especially HDO and it will produce more branched green diesel with good cold point characteristics due to the isomerization process [6], [7]. Green diesel offers a promising alternative to petroleum-based diesel due to its lower carbon footprint than commercial biofuels, abundant raw materials, and non-polluting production process. However, the high-pressure reactor required for green diesel production can significantly increase costs. To make green diesel a more economically viable option, developing a cheap and high-conversion heterogeneous catalyst is crucial [8].

The use of a suitable type of catalyst for the deoxygenation process is one of the most important parameters. Noble metals such as Pd, Pt, Ru, Rh, Ir and Os are the best types of catalysts today. Research that has been done shows that Pd and Pt with catalyst support from activated carbon have the highest DO activity in the DO reaction process with stearic acid as raw material [9]. The results of the study of Silva *et al*., showed the success of using a Pd/C catalyst in the deoxygenation reaction of macauba pulp and almond oil with hydrogen in the reaction. Deoxygenation at 300 °C and 10 bar hydrogen pressure yielded a product distribution of the majority of green diesel, then green aviation turbine fuel (avtur), and a minor fraction of green gasoline after 5 h [10].

Although it can show a high catalytic activity, the use of noble metals as catalysts is quite expensive if applied on an industrial scale. As an alternative, transition metals Ni and Cu are cheaper metals and can produce high yields and conversions in the DO process. In research done by Ambursa *et al*., the use of bimetallic Cu-Ni catalysts with MCM-41 and Ti-MCM-41 catalyst supports in the HDO process, which is a type of DO reaction with lignin as raw material, can produce high quality hydrocarbon products with 91.49% conversion and 50.09% selectivity of cyclohexane [11]. Another study showed that the use of different types of catalyst supports (γ-Al_2O_3, ZrO_2, and SiO_2) on Ni metal catalysts for deoxygenation reactions made from palm oil will result in a different distribution of green diesel products with the highest product in green diesel. They found that the Ni/Al_2O_3 catalyst exhibited the highest performance in the production of C_{17} hydrocarbons. With a conversion rate exceeding 90% and a C_{17} hydrocarbon yield of over 50% [12]. Another study also showed the use of Ni metal on Zeolite Y catalyst support exhibited the highest conversion of 76.21% and hydrocarbon selectivity of 84.28% when compared to other metals such as Cu, Co, Zn, Mn in the triolein deoxygenation reaction [13]. While significant progress has been made in catalyst development for green diesel production, the manufacture of catalysts with high activity for green diesel production still faces challenges, especially increasing selectivity and conversion.

In addition, the catalyst support plays an important role because it functions as a place for active metal dispersion to avoid sintering on heterogeneous metal catalysts. Zeolite's Brønsted acidity has driven extensive exploration of its use as a catalyst support for the DO process. This acidity facilitates the hydrocracking of alkanes [14]. Acid sites on the catalyst support play an important role in removing oxygen from oxy-compounds through the dehydration process [15]. The presence of a high level of Brönsted acidity on the zeolite affords active sites for coke production, causing the catalyst to deactivate [13], [16]. The incorporation of transition metals like Ni, Cu, and Zn into the zeolite framework was found to decrease coke formation. This effect is attributed to a reduction in the zeolite's Brønsted/Lewis acid site (B/L) ratio [13], [16], [17]. Consequently, a catalyst design that combines appropriate acidity on the support with well-dispersed metal sites can lead to enhanced hydrocarbon yields [18].

Indonesia has abundant mineral rock wealth, one of which is natural zeolite. There are many applications of natural zeolite such as industry, agriculture, to the waste treatment industry. In the industrial sector, natural zeolites are used as absorbents, catalysts, and separators of heavy metals [19]–[21]. Not many researchers have explored further the use of natural zeolite as a catalyst support in the deoxygenation process. The previous studies from Susanto *et al*., using Lampung zeolite (clinoptilolite type) as a support for Pd catalysts in the DO process with oleic acid as a model compound. This research

achieve a conversion value of 93.34%, a C_5–C_{25} selectivity of 63.68%, and a C_5–C_{25} yield of 52.685% at 350 °C and an H_2 pressure of 2 bar [22]. Other studies have also shown good conversion results using natural zeolite from Klaten, Central Java as an Fe support in the HDO process of refined palm oil. Metal loading on zeolite as much as 3 wt% succeeded in converting 89% of the raw material with the most products in the diesel range (C_{15}–C_{18}) [23]. Habibie, Susanto, and Carli (2018) used two types of metals Ni and Mo on natural zeolite catalyst supports from Malang for catalytic cracking reactions at atmospheric pressure, temperature 375 °C, for 1.5 h. The catalyst made is capable of converting oleic acid up to 84.30%, with product distribution in the form of biogasoline (23.08 wt%), bio jet fuel (36.43 wt%), renewable diesel (47.82 wt%), and lubricants (9.86 wt%) [24]. To the best of our knowledge, there is no report on Indonesia natural zeolite-supported nickel and copper used as catalysts for deoxygenation of fatty acid to produce green diesel. In this study, we synthesize single metallic and bimetallic nickel and copper supported on an activated Indonesia natural zeolite catalyst. The catalytic activity of synthesized catalysts in the deoxygenation of oleic acid to produce green diesel will be investigated. The green diesel product's composition will be studied as well. In addition, it will be studied further regarding the impact of changes in hydrogen pressure on the DO process on the resulting green diesel products.

2 Materials and Method

2.1 *Materials*

The metal precursor consists of nickel (II) nitrate hexahydrate and cooper (II) nitrate hexahydrate were purchased from Merck. Another material used is natural zeolite from Sukabumi, Indonesia. Oleic acid used for a model compound with decane as a solvent for the deoxygenation reaction was purchased from Sigma Aldrich. All reagents were used as received without further purification.

2.2 *Natural zeolite activation*

Natural zeolite from Sukabumi was crushed using a mortar. The refined natural zeolite was then homogenized using a 100-mesh sieve test. Subsequently, natural zeolite was soaked in deionized water and stirred for 24 h using a magnetic stirrer. The natural zeolite was then filtered and dried in an oven at 105 °C for 1 h. Natural zeolite was activated using acid activation method by soaking and stirring with 3M HCl solution at 50 °C for 1 h. After that, the natural zeolite was filtered and rinsed to pH 7, then heated in a furnace at 500 °C for 3 h.

2.3 *Catalyst synthesis*

Three kinds of activated natural zeolite-supported metal oxides were synthesized: activated natural zeoilite-supported nickel (Ni/ANZ), activated natural zeoilite-supported copper (Cu/ANZ), and activated natural zeoilite-supported mixture of nickel and copper (NiCu/ANZ). The catalyst was prepared by wet impregnation method using reflux, 10 g of activated natural zeolite was impregnated in $Ni(NO_3)_2.6H_2O$ (3 wt%) precursor which had been dissolved in 50 mL distilled water. The solution was stirred using a stirring bar at 70 °C for 4 h. The impregnation results were reheated using a furnace at a temperature of 105 °C for 24 h. The resulting powder was calcined under atmospheric air for 2 h at 500 °C with a heating rate of 10 °C/min and followed by reduction under hydrogen flow for 4 h at 500 °C with a heating rate of 5 °C/min. A similar method was used for the preparation of Cu/ANZ. In the preparation of NiCu/ANZ, the weight ratio of Ni/Cu is 1:1 with the total weight of metal at 3% of the activated natural zeolite.

2.4 *Catalyst characterization*

The elemental composition of natural zeolite before and after activation was analyzed using the XRF (X-ray Fluorescence) method with the PUMA - Bruker S2 tool. The measurement method uses SMART-Oxides with helium gas conditions. Identification of the crystalline phase of all catalysts was tested using XRD Rigaku SmartLab. All samples were prepared standardly on a special powder no height alignment holder using the BB (Bragg Bentano) scan method. Range at 2θ from 10°–90° and scan speed 5°/min with step width: 0.01 deg. The raw data is processed using the Match 3 application to determine the type of peak from the XRD data. The NH_3-TPD analysis was carried out with ChemiSorb 2750 Micromeritics to measure the number of acid sites and the acidity strength of the catalyst. Sample pretreatment was carried out by heating at 350 °C for 60 min under He gas (inert). The process was continued by adsorption of NH3 (5% in He, v/v) carried out at 100 °C for 30 min, then purging with He gas (inert) at the same

temperature, for 30 min. The final stage is the NH_3 desorption process, which is carried out at a temperature of 100–700 °C heating rate of 10 °C/min, then held for 15 min at the temperature of 700 °C. Nitrogen adsorption-desorption isotherms were obtained by measuring using a Micromeritics apparatus. Calculation of the specific surface area based on the BET equation using adsorption data recorded at a relative pressure range of $0.03 < P/P0 < 0.5$. The pore size distribution was determined using the BJH method and the N_2 desorption curve. Analysis of the morphological and particle size of the catalyst using SEM (Scanning Electron Microscope) at a magnification of 1000 times and 5000 times. EDX (Energy Dispersive X-ray) is used to determine the elemental composition on the surface of the catalyst.

2.5 *Deoxygenation of fatty acid*

The deoxygenation of oleic acid is carried out in a 160 mL autoclave batch reactor equipped with a magnetic stirrer. In typical reaction condition, a mixture of oleic acid (0.5 g), decane (24.5 g), and catalyst (0.025 g) were added to the reactor. Before the reaction starts, the reactor is purged twice using H_2 to clean the reactor and charged with 40 bar of H_2 at room temperature. The reaction was carried out at 350 °C for 3 h. After the reaction, the reactor was cooled to room temperature. Subsequently, the liquid product was analyzed by gas chromatography–mass spectrometry.

2.6 *Analysis of green diesel product*

The liquid product resulting from the deoxygenation reaction was analyzed using GC-MS Agilent 7890A with an HP-5MS column. The sample was mixed with the internal standard in the form of eugenol in a ratio of 10 mL of the sample added with 10 µL of eugenol. The sample was then derivatized so that non-volatile compounds could be analyzed on GC-MS. The derivatization procedure was started by taking a 50 µL sample and putting it in a 2 mL vial. The sample was mixed with 400 µL of DCM (dichloromethane) and added as much as 50 µL of BSTFA. The sample was then ignited at a temperature of 60–70 °C for 30 min. After 30 min, the sample was added again with 300 L of DCM, and the sample was ready for analysis. Conversion and Normalized % GC area by internal standard can be calculated by the following Equations (1) and (2).

$$\text{Conversion (\%)} = \frac{\text{NA Oleic Acid}_{\text{feed}} - \text{NA Oleic Acid}_{\text{products}}}{\text{NA Oleic Acid}_{\text{feed}}} \text{ x } 100\% \quad (1)$$

$$\text{Normalized \% Area GC} = \frac{\text{Area \% GC product}}{\text{Area \% GC of internal standard}} \quad (2)$$

*NA = Normalized % Area GC

3 Results and Discussion

3.1 *Catalyst characterization*

The objective of natural zeolite activation using HCl is to remove metal impurities, thus creating more porous and increasing the surface area of natural zeolite as well [25]. A summary of each element present in natural zeolite before and after activation is summarized in Table 1 with silica (Si) and aluminum (Al) are the main elements of natural zeolite. It can be seen in Table 1 that the activation process succeeded in removing impurity compounds that cover the surface and pores of the natural zeolite. The presence of non-optimal aluminum concentration in natural zeolite can act as a contaminant, leading to the formation of coke when used as a catalyst. Hence, this dealumination process aims to eliminate inactive skeleton aluminum from natural zeolite, enhancing its selectivity, acidity control, and stability during high-temperature reactions [26].

Table 1: Chemical composition of natural zeolite before and after activation.

Metal Element	Concentration (wt%)	
	Natural Zeolite	Activated Natural Zeolite
O	49.8	50.80
Na	1.00	0.40
Mg	0.70	0.40
Al	7.60	6.50
Si	35.00	37.90
P	0.20	0.20
S	0.10	0.10
Cl	0.10	0.20
K	2.50	1.70
Ca	1.50	1.10
Ti	0.10	0.10
Fe	1.30	0.50
Sr	0.10	0.10
Si/Al Mole Ratio	**4,424**	**5,602**

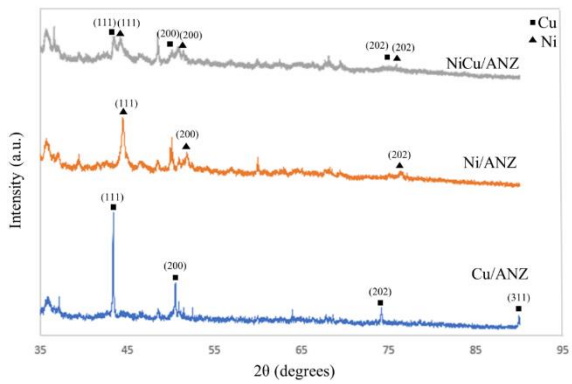

Figure 1: XRD pattern of catalyst.

The XRD patterns of the three catalyst types are shown in Figure 1. The appearance of XRD peaks at 43.3°, 50.4°, 74.1°, and 89.9° revealed the metallic cooper with the face center-cubic (fcc) structure Cu^0 that came from the reduction of catalyst Cu/ANZ, corresponding to (111), (200), (202), and (311) (JCPDS No. 04-0836) [27], [28]. The appearance of XRD peaks at 44.3°, 51.7°, and 76.1° at 2θ revealed the formation of elemental Ni in the reduced catalyst. The plane of (111), (200), and (202) indexed as reflections of metallic cubic Ni in Ni/ANZ catalyst (JCPDS No. 01-070-1849) [29], [30]. These findings indicate that the metals Ni and Cu have been successfully impregnated on the catalyst support. In the sample of the NiCu/ANZ bimetallic catalyst, there were peaks at 2θ = 43.4°, 50.6°, 74.3° which indicated the presence of Cu metal and peaks at 2θ = 44.1°, 51.4°, 75.7° which indicated the presence of Ni metal. There is no sign of peak shown NiCu alloy in the NiCu/ANZ. This shows that the monometallic Ni and Cu were incorporated together without forming the alloy material in this catalyst. As seen from the intensity of each peak, the peaks in the metals Ni and Cu decreased in the bimetallic catalyst when compared to the monometallic Cu and Ni catalysts. All metals impregnated on the catalyst support have a cubic crystal system.

The NH_3-TPD experiments were carried out to investigate the acid site concentration and properties. As shown in Table 2, the total acid sites of natural zeolite were decreased after activation using HCl. The acidity of the zeolite depends on the Si/Al atomic ratio. The number of Brönsted acid sites is proportional to the number of Al active atoms. Thus, the higher Si/Al ratio, the lower the acidity of the zeolite [31]. Although activated natural zeolite has a higher total acidity than catalysts impregnated with transition metals Ni and Cu, ANZ has a lot of strong acids, which indicates more Brönsted acid in zeolite. This will result in the formation of coke and deactivation of the catalyst, causing low conversion in the deoxygenation reaction [13], [16], [32]. However, weak and medium acid sites indicate the presence of Lewis acid sites in the catalyst [17]. Furthermore, the total acid sites in all samples were decreased when the metal was added. A similar finding was reported by Iliopoulou *et al*., and Kumar *et al*., where the addition of excessive Cu or Ni metal loading during the impregnation process led to the decrease of Brönsted acid sites, hence reducing the total acidity of catalyst [17], [33].

Table 2: Acidity of catalyst.

Catalyst	Total Acid (mmol/g)	Acidity		
		Weak	Medium	Strong
NZ*	0.95	1.132	0.424	0
ANZ**	0.69	0.688	0.587	0.21
Cu/ANZ	0.61	0.574	0.585	0.15
Ni/ANZ	0.56	0.572	0.509	0.007
NiCu/ANZ	0.55	0.514	0.366	0.027

*Natural Zeolite
**Activated Natural Zeolite

NH_3–TPD experiments were conducted to investigate the acid site concentration and properties. The results indicate the presence of weak acids (T < 250 °C) and strong acids (T > 500 °C), and the medium acidity was in the middle of this range [34]. The disparity in the number of weak acid sites between Cu/ANZ and Ni/ANZ is minimal, with NiCu/ANZ showing even lower levels compared to the other two catalysts. This can be attributed to the absence of Ni metal in the catalyst, which serves as Lewis Acid sites [35]. NiCu/ANZ exhibits significantly lower medium acid content compared to the other two catalysts. Cu/ANZ has the highest strong acid content at 0.15, followed by NiCu/ANZ at 0.027 and Ni/ANZ at 0.007. This disparity is attributed to the ability of Ni metal to substantially reduce the B/L ratio in ANZ compared to Cu metal, consistent with findings from Choo *et al*., [13]. The NiCu/ANZ catalyst exhibits a higher concentration of strong acid sites compared to Ni/ANZ, attributed to the inclusion of Cu metal.

As expected the surface area of natural zeolite is increased from 77.86 m^2/g to 84.65 m^2/g after activated with HCl as shown in Table 3. This increase was due to the activation process that succeeded in reducing impurities on the catalyst surface as already shown in Table 1. The pore diameter increased slightly from 14.07 nm to 14.63 nm. This is caused by the activation process that causes changes in the pore

structure of the natural zeolite. The addition of Ni and Cu caused the specific surface area to become smaller compared to activated natural zeolite. However, the mean pore diameters of all catalysts were higher than activated natural zeolite. This may be caused by the presence of solid metal material on the outer surface or deposited in the pores of catalyst support. This is similar to the result of Yang *et al.* [36], and Li *et al.* [37].

Table 3: Specific surface area and pore diameter of catalyst.

Catalyst	Specific Surface Area[a] (m^2/g)	Pore Diameter[b] (nm)
NZ*	77.9	14.1
ANZ**	84.7	14.6
Cu/ANZ	53.1	19.6
Ni/ANZ	76.4	16.0
NiCu/ANZ	75.0	18.3

*Natural Zeolite
**Activated Natural Zeolite
[a]BET Surface Area
[b]BJH Adsorption

Among activated natural zeolite-supported metals, Ni/ANZ catalyst has the highest specific surface area of 76.4 m^2/g, followed by NiCu/ANZ (74.9 m^2/g) and the lowest is Cu/ANZ (53.1 m^2/g). This could be due to more amount of Cu metal that binds in the ANZ support. Besides ionic bonding between Cu and zeolite, the ligated copper complexes are included in the pores and cages of zeolites because of the covalent delocalization between copper and oxygen [38]. However, between Ni and zeolite only the most ionic bonds occur. All catalysts experienced an increase in pore diameter and pore volume after the addition of Ni and Cu metals, except for the Ni/ANZ catalyst, which had lower pore volume than the catalyst support. Ni/ANZ catalyst has a smaller pore volume and pore diameter than the other two catalysts.

The results of the morphological analysis of the catalyst with SEM can be seen in Figure 2. The three catalysts have an amorphous shape with uneven sizes which can be seen in the image with a magnification of 1000 and 5000 times. On the Cu/ANZ catalyst (Figure 2(b)), some particles were seen on the surface, but it was not certain whether the particles were Cu metal or impurities that were still present on the surface of the zeolite. The particle image captured on the SEM is about ~75 µm in size. In the Ni/ANZ catalyst (Figure 2(d)), the same thing was seen with the particle size caught of ~40 µm. On the surface of the NiCu/ANZ catalyst, it is not much different from the particle size captured by ~60 µm.

The results of elemental analysis on the catalyst surface with EDX are presented in Figure 3. The Cu content in the Cu/ANZ catalyst is 3.8 wt%. This value exceeds the amount of impregnated catalyst, this because the high Cu loading make the formation of larger particle in the zeolite surface and decrease the dispersion of metal in the surface [39]. In addition, this exceeded value could be attributed to the lower surface area of the Cu/ANZ catalyst. The amount of Ni on the surface of the Ni/ANZ catalyst is almost half smaller than the initial metal loading amount, which is only 1.8 wt%. This phenomenon could be attributed to poor dispersion resulting from agglomeration during the drying and calcination stages in the wet impregnation method in the certain areas with reduced Ni particle presence on the surface were detected. In the NiCu/ANZ catalyst there is more Ni metal by 1.1 wt% than Cu metal by 0.8 wt% on the catalyst surface. This is because Ni has a smaller particle size compared to Cu, it exhibits better dispersion on the activated natural zeolite support [40]. This finding aligns with Kumar *et al*., research, which also demonstrated better Ni dispersion on zeolite supports [41].

3.2 *Deoxygenation of oleic acid*

3.2.1 Possible reaction of oleic acid deoxygenation

The deoxygenation reaction pathway of oleic acid can be seen in Figure 4. The first possible reaction pathway is hydrogenation, in which hydrogen is consumed and oleic acid is converted to stearic acid. The following reaction is followed by three different types of deoxygenation. The first is hydrodeoxygenation, which converts stearic acid to octadecane with a byproduct of H_2O due to hydrogen re-consumption. Decarbonylation is the second reaction pathway, which results in heptadecene products with CO and H_2O byproducts. If heptadecene is hydrogenated again, it will become heptadecane. The third reaction pathway is decarboxylation, which produces a heptadecane product with CO_2 as a byproduct. Due to the reaction conditions of high enough temperature and long time, heptadecane was converted into pentadecane and hexadecane via the hydrocracking reaction pathway. The octadecene product is formed from a dehydration reaction because it produces H_2O byproducts without consuming hydrogen. Octadecene undergoes hydrogenation to yield octadecane. However, the acidic nature of the catalyst support can promote a competing dehydration pathway. This is likely due to the ability of the acidic

sites to facilitate the removal of oxygen-containing functional groups. Subsequently, the exposed double bonds can then be hydrogenated by the Lewis acid sites on the metal component of the catalyst [15], [42]. The combination of acid sites on the natural zeolite catalyst support and good metal distribution on the catalyst surface gives high yields for the HDO product, namely octadecane [18].

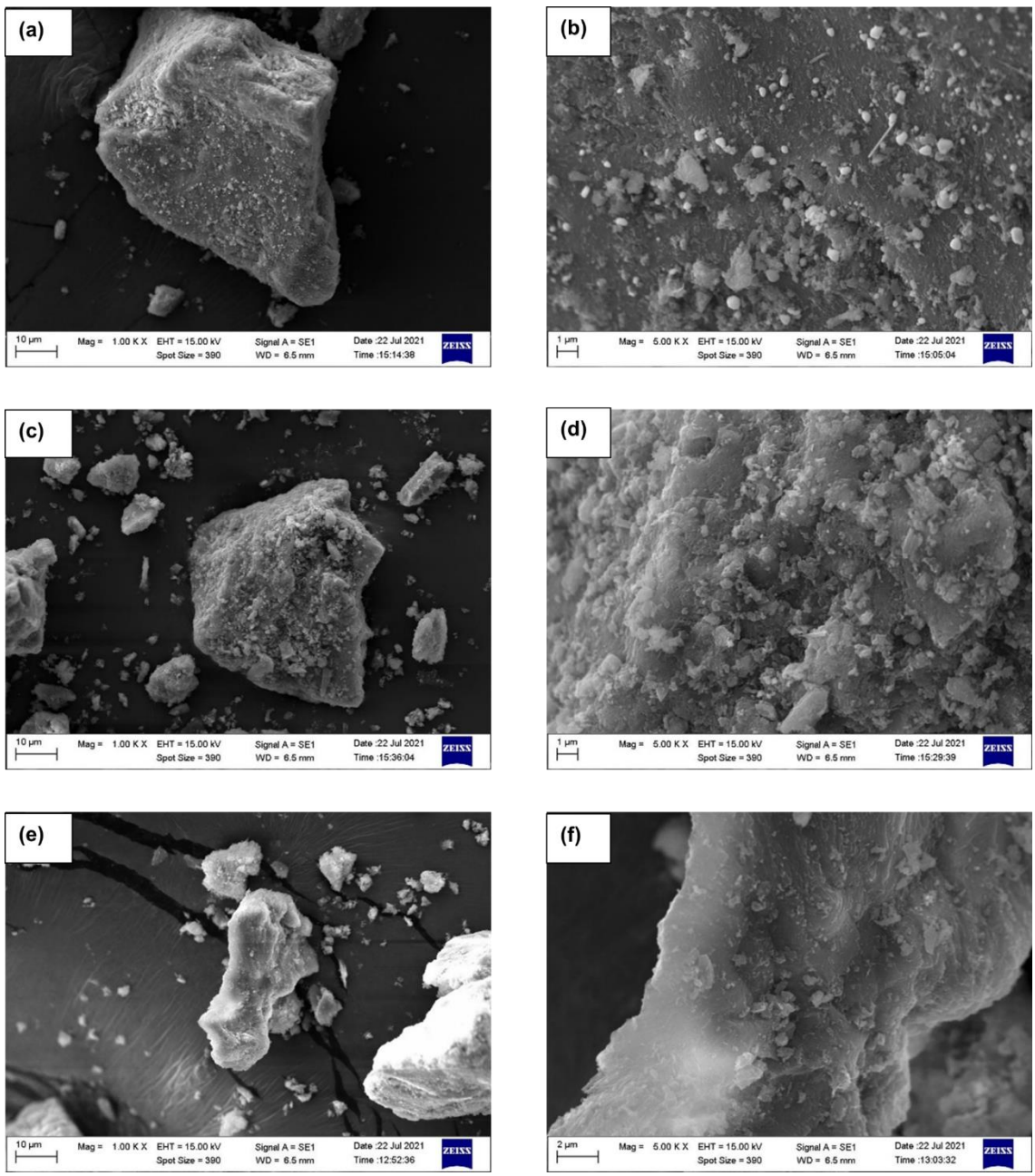

Figure 2: Catalyst Morphology from SEM (a) Cu-ANZ 1000x Mag, (b) Cu-ANZ 5000x Mag, (c) Ni-ANZ 1000x Mag, (d) Ni-ANZ 5000x Mag, (e) NiCu-ANZ 1000x Mag, (f) NiCu-ANZ 5000x Mag.

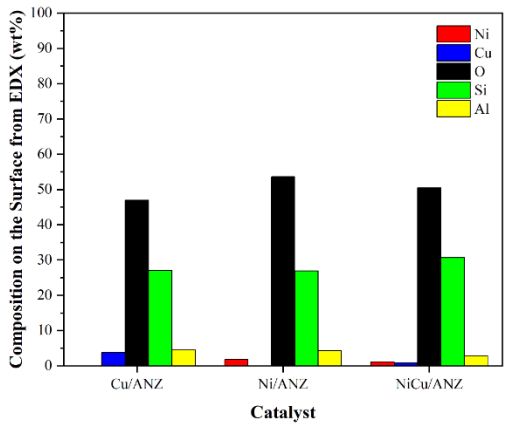

Figure 3: Results of elemental analysis on catalyst surface with EDX.

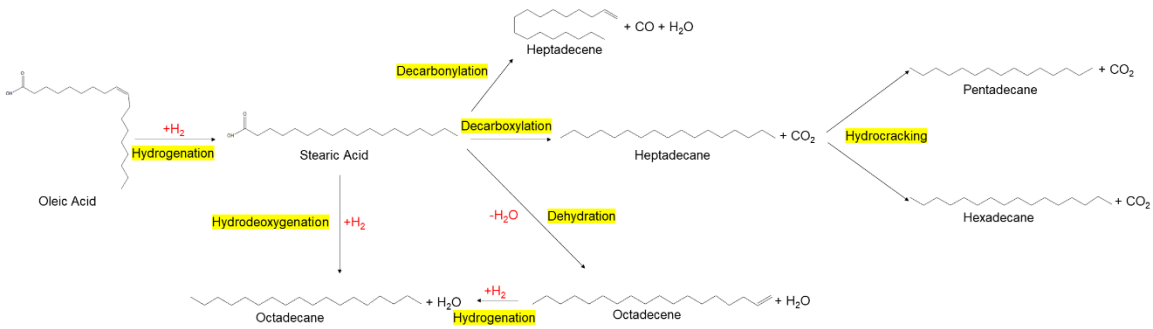

Figure 4: Oleic acid deoxygenation reaction pathway.

3.2.2 Effect of metal type on catalyst

The conversion value of oleic acid in the deoxygenation reaction is calculated using Equation (1) and the results can be seen in Figure 5. The highest conversion was obtained with the use of Cu/ANZ catalyst of 97.13%. Followed by the Ni/ANZ and NiCu/ANZ catalysts, with conversion values of 93.77% and 90.40%, respectively. The use of activated natural zeolite does not produce green diesel and has a low conversion value because there are no active acid sites on the metal. The conversion value obtained is directly proportional to the total acid of each catalyst. Cu/ANZ has the highest total acid of 0.61 mmol/g and the highest conversion of oleic acid, while NiCu/ANZ has the lowest total acid at 0.55 mmol/g and the lowest oleic acid conversion. We can conclude that the higher the total acid from the metal catalyst, the higher the conversion value of the oleic acid deoxygenation process. This study was similar to Cai *et al.*, the enhanced acidity of the catalyst will improve deoxygenation efficiency, reach a maximum catalyst activity, and increase the conversion [43].

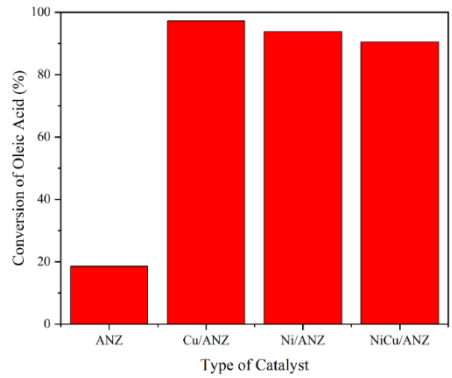

Figure 5: Oleic acid conversion in deoxygenation reaction from variation of catalyst type.

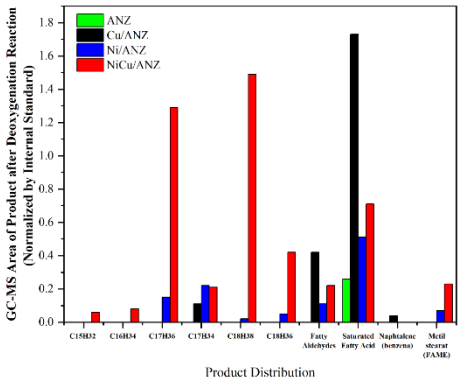

Figure 6: Distribution of deoxygenated products from oleic acid from variation of catalyst type.

The Cu/ANZ catalyst was able to produce the highest conversion value because the strong acid content was quite high compared to the other two catalysts. However, the yield of C_{15}–C_{18} products from the Cu/ANZ catalyst was the lowest compared to other catalysts as can be seen in Figure 6. The Cu/ANZ catalyst only creates heptadecene; the rest are byproducts of other organic molecules such as the fatty aldehydes group, saturated fatty acids or long chain fatty acids (LCFA), and a trace of benzene, namely naphthalene. This demonstrates that only decarbonylation and dehydrogenation reactions occur when the Cu/ANZ catalyst is used. These results are similar to the statement of Lup *et al.*, where decarbonylation and dehydrogenation are the two main reactions in the use of Cu metal as a catalyst in deoxygenation reactions [44].

Ni/ANZ catalyst has a variety of green diesel products from heptadecane, heptadecene, octadecane, and octadecene. This catalyst exhibits a significantly lower green diesel yield compared to the NiCu/ANZ catalyst. In fact, the conversion value of oleic acid from Ni/ANZ is higher than NiCu/ANZ. The best reason is the majority of Ni/ANZ products are gas products or short chain hydrocarbons due to excessive cracking reactions. This is indicated by the weight of the deoxygenation reaction using Ni/ANZ, which decreased to 17 g from the previous weight of 25 g. Based on the resulting product, the reaction pathways that occur in Ni/ANZ catalyst are decarbonylation, decarboxylation, hydrodeoxygenation, and dehydration. The HDO/deCO$_x$ ratio of the Ni/ANZ catalyst is 0.054, which indicates the deoxygenation reaction pathway that occurs is dominated by decarbonylation and decarboxylation reactions. Other studies have also stated the same thing, where the use of Ni metal as a monometallic catalyst will cause more HDO reactions to hydrogenation and deCO$_x$ [45].

The total green diesel product produced from the NiCu/ANZ catalyst was higher than that of the Ni/ANZ catalyst. The variety of green diesel products produced from the NiCu/ANZ catalyst is more than the Ni/ANZ catalyst because only a few products turn into gas and in the presence of hexadecane and pentadecane in the product. This shows that the use of a NiCu/ANZ catalyst does not only result in a deoxygenation reaction, but also a cracking reaction that is not excessive. Bimetallic nickel-based catalysts have been noted to have better deoxygenation performance due to the synergistic effect of other metals [44]. The combination of two metals Ni and Cu showed increased selectivity for long-chain hydrocarbons (C_{15}–C_{17}) produced from the DO process compared to using only one metal [46], [47]. The HDO/deCO$_x$ ratio of the NiCu/ANZ catalyst was 0.993 which indicated that the HDO reaction on the NiCu/ANZ catalyst was more dominant than the monometallic catalysts, Ni/ANZ and Cu/ANZ. A higher HDO/deCOx ratio is advantageous for the efficient production of octadecane. Conversely, a lower ratio can lead to excessive cracking, resulting in a greater proportion of lower-chain hydrocarbons that are not categorized as green diesel, as illustrated in Figure 4. The NiCu/ANZ catalyst showed a higher green diesel yield than the Ni/ANZ catalyst despite lower total acidity. It can be done by the synergistic effect of Ni and Cu metal on the activated natural zeolite surface. H_2 molecules preferentially adsorb and dissociate on Ni active sites. The dissociated hydrogen species migrate to Cu active sites, creating vacancies on Ni. These vacancies can then adsorb additional H_2, leading to a continuous cycle of adsorption, dissociation, and desorption. The desorbed hydrogen species are available for catalytic hydrogenation reactions [48]. The presence of FAME products on the use of Ni/ANZ and NiCu/ANZ catalysts indicates that Ni metal can cause an esterification reaction in this oleic acid deoxygenation process.

3.2.3 Optimization on H_2 Initial Pressure

The optimization process was carried out using a NiCu/ANZ catalyst because the conversion value was not much different from that of the Ni/ANZ catalyst and the total green diesel product produced was higher than other catalysts. The conversion value of oleic acid using a NiCu/ANZ catalyst with variations in initial hydrogen pressure of 20 bar, 40 bar, and 60 bar can be

seen in Figure 7. The pressure during the reaction is one of the important parameters that can cause hydrogenation, isomerization, and cracking reactions [45]. The higher the hydrogen pressure used in the deoxygenation reaction, the higher the conversion value of oleic acid produced. The same results are also shown by the results of research from Ambursa *et al.* [11], Han *et al.* [42], Berenblyum *et al.* [45], and Yang *et al.* [49].

The conversion of oleic acid at a pressure of 20 bar reached 77.93% and the conversion of oleic acid at a pressure of 60 bar reached 100%. This is caused by high pressure causing a hydrogenation reaction that consumes more hydrogen to be converted into products. The total green diesel product also increases as the pressure of the hydrogen used in the deoxygenation reaction increases as shown in Figure 8. At a pressure of 20 bar, the only product produced was heptadecane, which indicated that only a decarbonylation reaction occurred. However, this very small amount of product can also be explained as many of the products become gases as the amount of final product is reduced to 18 grams from 25 g of reactants. At a pressure of 60 bar, the product contains only heptadecane with octadecene. The lack of product variation at 60 bar pressure is due to the direct deoxygenation reaction and the cracking reaction will be inhibited at high pressure. This fact can be explained by Le Chatelier's Principle, where changes in pressure will affect chemical equilibrium. If the pressure is increased, the equilibrium will shift in the direction of the larger mole [45], [49].

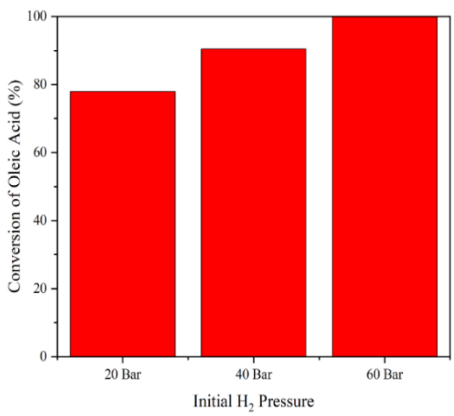

Figure 7: Effect of pressure on oleic acid conversion.

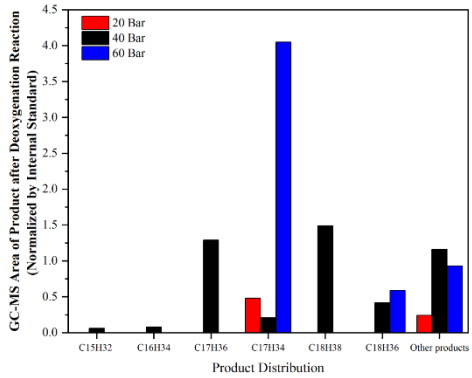

Figure 8: Distribution of deoxygenated products from oleic acid with NiCu/ANZ Catalyst in different H_2 initial pressures.

4 Conclusions

NiCu/ANZ is the best type of catalyst in this experiment seen from the high conversion value and the highest number of green diesel products in the deoxygenation reaction at a temperature of 350 °C, H_2 pressure of 40 bar, and a time of 3 h. Although the conversion of oleic acid is only 90.40%, which is slightly lower than the other two catalysts, the amount of green diesel product was relatively measured by the normalized percentage area of GC-MS. The result showed NiCu/ANZ yield 32 times and 4 times higher than Cu/ANZ and Ni/ANZ, respectively. The characteristics of the catalyst that determine the highest yield are high surface area and not too large total acid with the weakest acidity strength. If there are too many acid sites, it will cause an excessive cracking reaction so that more of the product becomes gas. Acidity strength that is too high also causes more product distribution to non-green diesel products. The greater the H_2 pressure will increase the conversion value of oleic acid and the amount of green diesel product in the reaction with a temperature of 350 °C, 3 h reaction. The best initial hydrogen pressure obtained in this study was 60 bar with the conversion value of oleic acid reaching 100% and the highest total green diesel product. This study highlights the potential of natural zeolite as a low-cost and sustainable catalyst support for green diesel production. By combining two non-noble metals with activated natural zeolite, the researchers developed a promising catalyst that demonstrated high conversion rates toward green diesel products. Further research is needed regarding the effect of other parameters such

as temperature, amount of catalyst, metal loading ratio, and deoxygenation reaction time.

Acknowledgments

We extend our sincere thanks to all who contributed to preparing the instructions. This research was funded by the KIST (Korea Institute of Science and Technology) School Project.

Author Contributions

G.H.A.W.: research design, methodology, data analysis, investigation, writing an original draft; F.S.H.S.: conceptualization, data curation, reviewing and editing, funding acquisition, project administration; A.A.D.: data curation, reviewing and editing. All authors have read and agreed to the published version of the manuscript.

Conflicts of Interest

The authors declare no conflict of interest.

References

[1] T. Wuttilerts, S. Chulalaksananukul, P. Peerapongpipat, and P. Suksommanat, "Evaluation of biodiesel production using oil feedstock from contaminated macro algae in shrimp farming," *Applied Science and Engineering Progress*, vol. 12, no. 3, pp. 179–185, 2019, doi: 10.14416/j.ijast.2018.11.005.

[2] S. Deshpande, A. Joshi, S. Vagge, and N. Anekar, "Corrosion behavior of nodular cast iron in biodiesel blends," *Engineering Failure Analysis*, vol. 105, pp. 1319–1327, 2019.

[3] S. Zulkepli, J. C. Juan, H. V. Lee, N. S. A. Rahman, P. L. Show, and E. P. Ng, "Modified mesoporous HMS supported Ni for deoxygenation of triolein into hydrocarbon-biofuel production," *Energy Conversion and Management*, vol. 165, pp. 495–508, 2018.

[4] N. Asikin-Mijan, H. V. Lee, J. C. Juan, A. R. Noorsaadah, G. Abdulkareem-Alsultan, M. Arumugam, Y. H. Taufiq-Yap, "Waste clamshell-derived CaO supported Co and W catalysts for renewable fuels production via cracking-deoxygenation of triolein," *Journal of Analytical and Applied Pyrolysis*, vol. 120, pp. 110–120, 2016.

[5] S. L. Douvartzides, N. D. Charisiou, K. N. Papageridis, and M. A. Goula, "Green diesel: Biomass feedstocks, production technologies, catalytic research, fuel properties and performance in compression ignition internal combustion engines," *Energies*, vol. 12, p. 809, 2019.

[6] E. S. de Almeida, D. da Silva Damaceno, L. Carvalho, P. A. Victor, R. M. Dos Passos, P. V. de Almeida Pontes, M. Cunha-Filho, K. A. Sampaio, S. Monteiro, "Thermal and physical properties of crude palm oil with higher oleic content," *Applied Sciences*, vol. 11, p. 7094, 2021.

[7] F. P. Sousa, L. N. Silva, D. B. de Rezende, L. C. A. de Oliveira, and V. M. D. Pasa, "Simultaneous deoxygenation, cracking and isomerization of palm kernel oil and palm olein over beta zeolite to produce biogasoline, green diesel and biojet-fuel," *Fuel*, vol. 223, pp. 149–156, 2018.

[8] H. I. Mahdi, A. Bazargan, G. McKay, N. I. W. Azelee, and L. Meili, "Catalytic deoxygenation of palm oil and its residue in green diesel production: A current technological review," *Chemical Engineering Research and Design*, vol. 174, pp. 158–187, 2021.

[9] M. Snåre, I. Kubičková, P. Mäki-Arvela, K. Eränen, and D. Y. Murzin, "Heterogeneous catalytic deoxygenation of stearic acid for production of biodiesel," *Industrial and Engineering Chemistry Research*, vol. 45, no. 16, pp. 5708–5715, 2006.

[10] L. N. Silva, I. C. P. Fortes, F. P. De Sousa, and V. M. D. Pasa, "Biokerosene and green diesel from macauba oils via catalytic deoxygenation over Pd/C," *Fuel*, vol. 164, pp. 329–338, 2016.

[11] M. M. Ambursa, P. Sudarsanam, L. H. Voon, S. B. A. Hamid, and S. K. Bhargava, "Bimetallic Cu-Ni catalysts supported on MCM-41 and Ti-MCM-41 porous materials for hydrodeoxygenation of lignin model compound into transportation fuels," *Fuel Processing Technology*, vol. 162, pp. 87–97, 2017.

[12] K. N. Papageridis, N. D. Charisiou, S. L. Douvartzides, V. Sebastian, S. J. Hinder, M. A. Baker, S. Alkhoori, K. Polychronopoulou, M. A. Goula, "Effect of operating parameters on the selective catalytic deoxygenation of palm oil to produce renewable diesel over Ni supported on $A_{l2}O_3$, ZrO_2 and SiO_2 catalysts," *Fuel Processing Technology*, vol. 209, 2020, Art. no. 106547.

[13] M. Y. Choo, L. E. Oi, T. C. Ling, E. P. Ng, Y. C. Lin, G. Centi, J. C. Juan, "Deoxygenation of triolein to green diesel in the H2-free condition: Effect of transition metal oxide supported on zeolite Y," *Journal of Analytical and Applied Pyrolysis*, vol. 147, p. 104797, 2020.

[14] A. E. Coumans and E. J. M. Hensen, "A real support effect on the hydrodeoxygenation of methyl oleate by sulfided NiMo catalysts," *Catalysis Today*, vol. 298, pp. 181–189, 2017.

[15] O. U. Valdés-Martínez, V. A. Suárez-Toriello, J. A. de los Reyes, B. Pawelec, and J. L. G. Fierro, "Support effect and metals interactions for NiRu/Al_2O_3, TiO_2 and ZrO_2 catalysts in the hydrodeoxygenation of phenol," *Catalysis Today*, vol. 296, pp. 219–227, 2017.

[16] D. Yao, H. Yang, H. Chen, and P. T. Williams, "Investigation of nickel-impregnated zeolite catalysts for hydrogen/syngas production from the catalytic reforming of waste polyethylene," *Applied Catalysis B: Environmental*, vol. 227, pp. 477–487, 2018.

[17] R. Kumar, V. Strezov, E. Lovell, T. Kan, H. Weldekidan, J. He, S. Jahan, B. Dastjerdi, J. Scott, "Enhanced bio-oil deoxygenation activity by Cu/zeolite and Ni/zeolite catalysts in combined in-situ and ex-situ biomass pyrolysis," *Journal of Analytical and Applied Pyrolysis*, vol. 140, pp. 148–160, 2019.

[18] T. L. R. Hewer, A. G. F. Souza, K. T. C. Roseno, P. F. Moreira, R. Bonfim, R. M. B. Alves, M. Schmal, "Influence of acid sites on the hydrodeoxygenation of anisole with metal supported on SBA-15 and SAPO-11," *Renewable Energy*, vol. 119, pp. 615–624, 2018.

[19] M. Al-Muttaqii, F. Kurniawansyah, D. H. Prajitno, and A. Roesyadi, "Bio-kerosene and bio-gasoil from coconut oils via hydrocracking process over Ni-Fe/HZSM-5 catalyst," *Bulletin of Chemical Reaction Engineering & Catalysis*, vol. 14, no. 2, pp. 309–319, 2019.

[20] G. A. Bani and M. D. Bani, "Pyrolysis of polyethylene from plastic waste using activated ende natural zeolite as a catalyst," *Applied Science and Engineering Progress*, vol. 17, no. 2, 2024, Art. no. 7320, doi: 10.14416/j.asep. 2024.01.006.

[21] B. Wongchalerm, T. Arunchai, T. Khamkenbong, S. Sangsuradet, A. Pitiraksakul, and P. Worathanakul, "Simulation and experimental studies on sustainable process optimization of CO_2 adsorption using zeolite 5A pellet," *Applied Science and Engineering Progress*, vol. 16, no. 2, 2022, Art. no. 5861, doi: 10.14416/j.asep.2022.04.004.

[22] B. H. Susanto, M. Nasikin, Sukirno, and A. Wiyo, "Synthesis of Renewable Diesel through Hydrodeoxygenation Using Pd/zeolite Catalysts," *Procedia Chemistry*, vol. 9, pp. 139–150, 2014.

[23] R. Putra, W. W. Lestari, F. R. Wibowo, and B. H. Susanto, "Fe/Indonesian natural zeolite as hydrodeoxygenation catalyst in green diesel production from palm oil," *Bulletin of Chemical Reaction Engineering & Catalysis*, vol. 13, no. 2, pp. 245–255, 2018.

[24] T. K. Habibie, B. H. Susanto, and M. F. Carli, "Effect of NiMo/Zeolite catalyst preparation method for bio jet fuel synthesis," in *E3S Web of Conferences*, Nov. 2018, p. 02024.

[25] X. Guo, L. Guo, Y. Zeng, R. Kosol, X. Gao, Y. Yoneyama, G. Yang, N. Tsubaki, "Catalytic oligomerization of isobutyl alcohol to jet fuels over dealuminated zeolite Beta," *Catalysis Today*, vol. 368, pp. 196–203, 2021.

[26] S. Gea, A. Haryono, A. Andriayani, J. L. Sihombing, A. N. Pulungan, T. Nasution, R. Rahayu, Y. A. Hutapea, "The stabilization of liquid smoke through hydrodeoxygenation over nickel catalyst loaded on sarulla natural zeolite," *Applied Sciences*, vol. 10, p. 4126, 2020.

[27] H. Du, X. Ma, P. Yan, M. Jiang, Z. Zhao, and Z. C. Zhang, "Catalytic furfural hydrogenation to furfuryl alcohol over Cu/SiO2 catalysts: A comparative study of the preparation methods," *Fuel Processing Technology*, vol. 193, pp. 221–231, 2019.

[28] X. Ma, H. Song, and J. Yan, "Electrochemically mediated gradient metallic film generation," *New Journal of Chemistry*, vol. 45, no. 4, pp. 1809–1813, 2021.

[29] A. Quindimil, U. De-La-Torre, B. Pereda-Ayo, A. Davó-Quiñonero, E. Bailón-García, D. Lozano-Castelló, J. A. González-Marcos, A. Bueno-López, J. R. González-Velasco, "Effect of metal loading on the CO_2 methanation: A comparison between alumina supported Ni and Ru catalysts," *Catal Today*, vol. 356, pp. 419–432, 2020.

[30] Q. Liu, F. Gu, X. Lu, Y. Liu, H. Li, Z. Zhong, G. Xu, F. Su, "Enhanced catalytic performances of Ni/Al_2O_3 catalyst via addition of V_2O_3 for CO

methanation," *Applied Catalysis A: General*, vol. 488, pp. 37–47, 2014.

[31] S. De, S. Dutta, and B. Saha, "Critical design of heterogeneous catalysts for biomass valorization: Current thrust and emerging prospects," *Catalysis Science and Technology*, vol. 6, no. 20, pp. 7364–7385, 2016.

[32] W. Yao, J. Li, Y. Feng, W. Wang, X. Zhang, Q. Chen, S. Komarneni, Y. Wang, "Thermally stable phosphorus and nickel modified ZSM-5 zeolites for catalytic co-pyrolysis of biomass and plastics," *RSC Advances*, vol. 5, no. 39, pp. 30485–30494, 2015.

[33] E. F. Iliopoulou, S. D. Stefanidis, K. G. Kalogiannis, A. Delimitis, A. A. Lappas, and K. S. Triantafyllidis, "Catalytic upgrading of biomass pyrolysis vapors using transition metal-modified ZSM-5 zeolite," *Applied Catalysis B: Environmental*, vol. 127, pp. 281–290, 2012.

[34] N. Asikin-Mijan, J. M. Ooi, G. AbdulKareem-Alsultan, H. V. Lee, M. S. Mastuli, N. Mansir, F. A. Alharthi, A. A. ALghamdi, Y. H. Taufiq-Yap, "Free-H2 deoxygenation of *Jatropha curcas* oil into cleaner diesel-grade biofuel over coconut residue-derived activated carbon catalyst," *Journal of Cleaner Production*, vol. 249, 2020, Art. no. 119381.

[35] H. Gao, L. Hu, Y. Hu, X. Lv, Y. B. Wu, and G. Lu, "Origins of Lewis acid acceleration in nickel-catalysed C-H, C-C and C-O bond cleavage," *Catalysis Science and Technology*, vol. 11, no. 13, pp. 4417–4428, 2021.

[36] M. Yang, J. Shao, Z. Yang, H. Yang, X. Wang, Z. Wu, H. Chen, "Conversion of lignin into light olefins and aromatics over Fe/ZSM-5 catalytic fast pyrolysis: Significance of Fe contents and temperature," *Journal of Analytical and Applied Pyrolysis*, vol. 137, pp. 259–265, 2019.

[37] C. Li, Nishu, D. Yellezuome, Y. Li, R. Liu, and J. Cai, "Enhancing bio-aromatics yield in bio-oil from catalytic fast pyrolysis of bamboo residues over bi-metallic catalyst and reaction mechanism based on quantum computing," *Fuel*, vol. 336, 2023, Art. no. 127158,

[38] P. Vanelderen, J. Vancauwenbergh, B. F. Sels, and R. A. Schoonheydt, "Coordination chemistry and reactivity of copper in zeolites," *Coordination Chemistry Reviews*, vol. 257, pp. 483–494, 2013.

[39] H. Mitta, P. K. Seelam, S. Ojala, R. L. Keiski, and P. Balla, "Tuning Y-zeolite based catalyst with copper for enhanced activity and selectivity in vapor phase hydrogenolysis of glycerol to 1,2-propanediol," *Applied Catalysis A: General*, vol. 550, pp. 308–319, 2018.

[40] B. Seemala, C. M. Cai, R. Kumar, C. E. Wyman, and P. Christopher, "Effects of Cu–Ni Bimetallic Catalyst Composition and Support on Activity, Selectivity, and Stability for Furfural Conversion to 2-Methyfuran," *ACS Sustainable Chemistry & Engineering*, vol. 6, pp. 2152–2161, 2017.

[41] R. Kumar, V. Strezov, E. Lovell, T. Kan, H. Weldekidan, J. He, B. Dastjerdi, J. Scott, "Bio-oil upgrading with catalytic pyrolysis of biomass using Copper/zeolite-Nickel/zeolite and Copper-Nickel/zeolite catalysts," *Bioresource Technology*, vol. 279, pp. 404–409, 2019.

[42] F. Han, Q. Guan, and W. Li, "Deoxygenation of methyl palmitate over SiO2-supported nickel phosphide catalysts: Effects of pressure and kinetic investigation," *RSC Advances*, vol. 5, no. 130, pp. 107533–107539, 2015.

[43] Z. Cai, R. Liang, P. Yu, Y. Liu, Y. Ma, Y. Cao, K. Huang, L. Jiang, X. Bao, "Improving conversion of methyl palmitate to diesel-like fuel through catalytic deoxygenation with B2O3-modified ZrO2," *Fuel Processing Technology*, vol. 226, 2022, Art. no. 107091.

[44] A. N. Kay Lup, F. Abnisa, W. M. A. Wan Daud, and M. K. Aroua, "A review on reactivity and stability of heterogeneous metal catalysts for deoxygenation of bio-oil model compounds," *Journal of Industrial and Engineering Chemistry*, vol. 56, pp. 1–34, 2017.

[45] Y. Yang, Q. Wang, X. Zhang, L. Wang, and G. Li, "Hydrotreating of C18 fatty acids to hydrocarbons on sulphided NiW/SiO2-Al2O3," *Fuel Processing Technology*, vol. 116, pp. 165–174, 2013.

[46] E. Santillan-Jimenez, R. Loe, M. Garrett, T. Morgan, and M. Crocker, "Effect of Cu promotion on cracking and methanation during the Ni-catalyzed deoxygenation of waste lipids and hemp seed oil to fuel-like hydrocarbons," *Catalysis Today*, vol. 302, pp. 261–271, 2018.

[47] Y. Li, C. Zhang, Y. Liu, S. Tang, G. Chen, R. Zhang, X. Tang, "Coke formation on the surface of Ni/HZSM-5 and Ni-Cu/HZSM-5 catalysts during bio-oil hydrodeoxygenation," *Fuel*, vol. 189, pp. 23–31, 2017.

[48] C. Miao, G. Zhou, S. Chen, H. Xie, and X. Zhang, "Synergistic effects between Cu and Ni species in NiCu/γ-Al_2O_3 catalysts for

hydrodeoxygenation of methyl laurate," *Renewable Energy*, vol. 153, pp. 1439–1454, 2020.

[49] A. S. Berenblyum, V. Y. Danyushevsky, E. A. Katsman, R. S. Shamsiev, and V. R. Flid, "Specifics of the stearic acid deoxygenation reaction on a copper catalyst," *Petroleum Chemistry*, vol. 53, no. 6, pp. 362–366, 2013.